Food Science of Animal Products

Research Article

Inhibition of α-amylase by sea cucumber intestinal collagen hydrolysates

Zhe Xu[1], Tengfei Li[1], Zijin Qin[2], Shuyu Zhou[1], Jianbo Sun[1], Xuguang Mo[1], Fuzhen Wang[1], Tingting Li[1] ✉

[1] *Key Laboratory of Biotechnology and Bioresources Utilization, Ministry of Education, College of Life Sciences, Dalian Minzu University, Dalian 116600, China*

[2] *Department of Food Science and Technology, University of Georgia, Athens 30602, USA*

✉Address correspondence to Tingting Li, jwltt@dlnu.edu.cn

Received: July 7, 2026; Revised: July 22, 2026; Accepted: July 30, 2026

Abstract: Starch digestion regulation is important for blood glucose control and weight management. α-Amylase inhibitors are one of major interventions for blood glucose reduction and weight management. Sea cucumber intestines are marine by-products with extensive bioactive compounds like collagen, however, research on their α-amylase inhibitory mechanisms remains limited. In this study, sea cucumber intestinal collagen hydrolysates (SCICHs) were generated by enzymatic hydrolysis (pepsin, neutral protease, and trypsin), and their interaction with α-amylase were investigated through spectroscopic and kinetic analysis. SCICHs were found to interact with α-amylase and assemble enzyme-hydrolysate complexes. Such interactions exhibited concentration-dependent behavior, progressively diminishing the catalytic activity of α-amylase while simultaneously eliciting conformational rearrangements in its secondary structure. The tryptic hydrolysate showed the highest inhibitory activity, achieving 64.71% inhibition rate comparable to the positive control (acarbose). Enzymatic kinetic analysis indicated that SCICHs suppress α-amylase activity via a reversible mixed-type inhibitory mode, which can bind to both the unbound enzyme and the enzyme-substrate complex, displaying a higher affinity toward the free enzyme. These findings imply that SCICHs possess the capacity to suppress α-amylase and hold potential as a natural constituent for formulating functional foods targeting obesity control.

Keywords: sea cucumber intestine; collagen hydrolysate; α-amylase; enzymatic inhibition; marine byproduct

Citation: Z. Xu, T. F. Li, Z. J. Qin, et al., Inhibition of α-amylase by sea cucumber intestinal collagen hydrolysates, Food Sci. Anim. Prod. 4 (2026) 9240190. https://doi.org/10.26599/FSAP.2026.9240190.

1 Introduction

Obesity has escalated into a worldwide public health crisis, posing substantial clinical hurdles due to its robust link to metabolic comorbidities, notably type 2 diabetes, cardiovascular pathologies, and malignancy[1]. As reported by World Health Organization, the global prevalence of obesity surpassed one billion in 2022, comprising 159 million youths aged 5–19 years and 879 million adults[2]. Current obesity management mainly focuses on energy restriction and metabolic enhancement, but overly restrictive diets may compromise both physical and psychological health[3]. Therefore, there is a need for effective and safe treatment options. α-Amylase catalyzes the hydrolysis of starch into smaller units, inducing elevated postprandial blood glucose levels. Excessive lipid accumulation in the body not only promotes the development of obesity but also further elevates blood glucose levels and disrupts metabolic homeostasis. α-Amylase inhibitors can inhibit enzyme activity, block carbohydrate hydrolysis, and thereby attenuate intestinal glucose absorption. Therefore, α-amylase inhibitors are expected to be applied in the intervention and improvement of postprandial blood glucose abnormalities[4].

In recent years, peptide-type inhibitors have emerged as a prominent research hotspot owing to their remarkable advantages including abundant raw material sources, well-defined inhibitory mechanisms and mild toxic and side effects. Valencia-Mejía et al.[5] reported that polypeptides extracted from legumes had inhibitory efficacy against α-amylase. de Matos et al.[6] also reported this inhibitory activity from black cricket protein hydrolysates. Marine-derived bioactive peptides usually refer to small peptides containing 2–20 amino acid residues and exhibiting distinct physiological activities. Because of their diverse origins, high biological selectivity, and favorable safety characteristics, increasing attention has been devoted to these compounds[6]. For example, it has been reported that hydrolysates prepared from shrimp shell by-products produced a 43.4% inhibition rate against α-amylase[7]. Similarly, Sintsova et al.[8] identified a β-defensin analogue purified from the mucus of *Heteractis magnifica*. This peptide exerted potent inhibitory activity against human pancreatic and salivary α-amylases at nanomolar concentrations, with outstanding thermostability and favorable biocompatibility.

Sea cucumbers belong to invertebrates that exist across diverse regions, and possess considerable development value for food and medicinal product research. They contain diverse bioactive compounds such as vitamins, minerals, cerebrosides, and peptides[9–10]. Moreover, sea cucumber collagen-derived peptides exhibit diverse biological activities, including antitumor effects, inflammation effects, immune enhancement, blood pressure and glucose modulation, anti-fatigue effects[11–12]. Currently, research on sea cucumbers primarily focuses on the extraction and preparation of bioactive peptide sequences and the investigation of their

© Beijing Academy of Food Sciences 2026. Food Science of Animal Products published by Tsinghua University Press. This is an open access article under the CC BY-NC-ND license (http://creativecommons.org/licenses/by-nc-nd/4.0/).

biological effects[9,11,13]. Intestinal tissues from sea cucumber processing constitute a substantial residue, harboring abundant bioactive substances encompassing unsaturated fatty acids, bioactive peptides, premium proteins, and amino acids. However, they are usually treated as processing by-product and discarded, resulting in significant resource waste[14]. Effective and rational utilization of these byproducts could add value of product processing. Sea cucumbers body wall peptides have been reported for digestive enzyme activity modulation. For example, Chen et al.[15] identified two α-amylase inhibitor peptides SCP1 and SCP2 from Russian sea cucumber peptides. These peptides inhibited the binding interaction between enzyme and substrate, resulting in interfered glycosylation process. However, research on α-amylase inhibitors derived from sea cucumber intestinal collagen remains relatively limited, with their specific inhibitory types and mechanisms of action yet to be fully elucidated.

This study aims to prepare α-amylase inhibitors with inhibitory activity by hydrolyzing sea cucumber intestinal collagen using pepsin, neutral protease, and trypsin. These enzymatic products hold promise as novel, natural and renewable α-amylase inhibitors for application in obesity and weight management, offering unique advantages including high market acceptability and low risk of drug resistance.

2 Materials and methods

2.1 Materials and chemicals

Fresh sea cucumber intestines were purchased from a food processing enterprise in Dalian, Liaoning Province, fully rinsed with deionized water, and stored frozen at −20 °C for subsequent use. Porcine pancreatic α-amylase (Cat. No. S31302, enzyme activity 10 U/mg), soluble starch and 3,5-dinitrosalicylic acid (DNS) reagent were obtained from Shanghai Yuanye Bio-Technology Co., Ltd. (Shanghai, China). Pepsin (Cat. No. S10029, enzyme activity 10 000 U/g), bovine pancreatic trypsin (Cat. No. S10032, enzyme activity 250 U/mg) and positive inhibitor acarbose were supplied by Shanghai Aladdin Biochemical Technology Co., Ltd (Shanghai, China). Neutral protease (Cat. No. Z8030, enzyme activity 60 000 U/g) was purchased from Beijing Solarbio Science & Technology Co., Ltd (Beijing, China). Sodium dihydrogen phosphate and disodium hydrogen phosphate were sourced from Tianjin Kemiou Chemical Reagent Co., Ltd (Tianjin, China). All other reagents adopted in this experiment were of analytical grade, and ultrapure water was utilized throughout all experimental operations.

2.2 Preparation of sea cucumber intestinal collagen hydrolysates (SCICHs)

Collagen from sea cucumber intestines was extracted according to the previously reported method[16]. The extracted collagen was dissolved in deionized water to yield a 20 mg/mL solution. The pH of the collagen solution was adjusted to the respective optimum for each enzyme using 1 mol/L HCl or 1 mol/L NaOH. Pepsin, trypsin, and neutral protease were separately added at a dosage of 5 000 U/g substrate protein. Enzymatic hydrolysis was performed for 5 h under continuous magnetic stirring at their respective optima: pH 2.0 and 37 °C for pepsin, pH 8.0 and 37 °C for trypsin, pH 7.0 and 50 °C for neutral protease. Following hydrolysis, the reaction was terminated by heating in a boiling water bath for 10 min. After cooling to room temperature, the mixtures were readjusted to neutral pH (7.0) and then centrifuged at 10 000 × g for 10 min at 4 °C. The supernatants were collected and stored at −20 °C for subsequent use, yielding three hydrolysates designated as SCIPH, SCITH, and SCINPH, respectively[17–18].

2.3 Fluorescence spectroscopy measurement

Following hydrolysate treatment, the fluorescence spectra of α-amylase were collected according to an earlier reported method with minor modifications[19]. The enzyme solution (4 U/mL) was combined with varying concentrations of hydrolysates and equilibrated at 298, 308, or 318 K for 1 h. Spectra were acquired on an LS55 spectrofluorometer (PerkinElmer, Waltham, MA, USA) with excitation at 280 nm, emission over 310–500 nm, slit width of 5 nm, and scan rate of 100 nm/min. Quenching data were interpreted using the Stern-Volmer equation (Eq. (1))[20]:

$$\frac{F_0}{F} = 1 + K_q \tau_0 [Q] = 1 + K_{sv} [Q] \quad (1)$$

Where F and F_0 represent the intrinsic fluorescence intensities of α-amylase in the presence and absence of hydrolysate, respectively; $[Q]$ denotes the concentration of the quencher, namely the hydrolysate, ranging from 0 to 800 μg/mL; K_{sv} represents the Stern-Volmer quenching constant (10^3 L/g); K_q refers to the bimolecular quenching rate constant (10^{11} L/(g·s)); and τ_0 is the mean fluorescence lifetime of the fluorophore (set as 10^{-8} s).

2.4 Circular dichroism (CD) spectrum measurement

CD was used to analyze α-amylase secondary structure changes caused by hydrolysates (Applied Photophysics, UK). Spectra were scanned at 190–260 nm with 0.2 nm slit width and 1 mm path length. Buffer background was subtracted from raw spectra to obtain the final data[21].

2.5 Inhibitory activity and mechanism of SCICHs against α-amylase

2.5.1 α-Amylase inhibitory activity measurement

DNS spectrophotometry was used to evaluate the inhibitory activities of SCIPH, SCITH, and SCINPH against α-amylase. In 0.2 mol/L phosphate buffer at pH 6.9, 4 U/mL enzyme solution was mixed with the three hydrolysates at concentrations of 1, 10, 100 and 1 000 μg/mL, acarbose was used as the positive control at the same concentration gradient (1, 10, 100 and 1 000 μg/mL), followed by pre-incubation at 37 °C for 10 min. Afterwards, 1 g/100 mL soluble starch was added, and the mixture was incubated at 37 °C for 5 min. Subsequently, 1 mL DNS reagent was added to terminate the reaction, and the mixture was heated in a boiling water bath for 10 min. After cooling to ambient temperature, the absorbance at 540 nm was recorded with a Synergy H1 hybrid multi-mode microplate reader (BioTek, Winooski, VT, USA). The inhibition rate was determined according to Eq. (2). Half maximal inhibitory concentration (IC_{50}) values were determined by relating the percentage inhibition of each sample to its concentration[22–23]:

$$\text{Inhibition rate}\ (\%) = (1 - \frac{B - b}{A - a}) \times 100 \quad (2)$$

Where A and a indicate the absorbance measured for the blank group (contains α-amylase and substrate (starch), but does not contain inhibitors) and blank control group (contains substrate (starch) but not contain α-amylase), respectively; B denotes the

absorbance of the system in which α-amylase was incubated with the SCICHs inhibitor, whereas *b* corresponds to the background control containing SCICHs alone without α-amylase.

2.5.2 *Inhibition kinetics of α-amylase by SCICHs*

The inhibitory kinetics of α-amylase by SCICHs were investigated through activity measurements under varying starch concentrations (1–8 mmol/L) and hydrolysate levels (1–1 000 μg/mL), maintaining an α-amylase content of 10 mg/mL[24].

Lineweaver-Burk plots were established by plotting the reciprocal of the reaction rate against the reciprocal of the substrate concentration. The inhibition type was identified by comparing the plots obtained at different hydrolysate concentrations. The kinetic equation was shown in Eq. (3)[25]:

$$v = \frac{v_{max}[S]}{K_m(1+\frac{i}{K_i})+[S](1+\frac{i}{K_{is}})} \quad (3)$$

Where v indicates initial reaction rate (min^{-1}); v_{max} indicates the maximum initial reaction rate achieved when all enzyme active sites are saturated with substrate (min^{-1}); i indicates inhibitor concentration (mg/mL); $[S]$ indicates substrate concentration (mmol/L); K_m indicates Michaelis-Menten constant (mmol/L); K_i indicates the equilibrium dissociation constant for inhibitor binding to free enzyme (mg/mL); and K_{is} refers to the equilibrium dissociation constant of inhibitor binding to the enzyme-substrate complex (mg/mL).

2.6 Statistical analyses

To ensure experimental reproducibility and data reliability, all tests were conducted in triplicate, and the results were presented as mean ± standard deviation (SD). One-way analysis of variance was employed to analyze inter-group differences, with Duncan's multiple range test applied for post-hoc comparisons. $P < 0.05$ was set as the threshold for statistical significance. Data analysis was performed using SPSS 27 (SPSS Inc., Chicago, IL, USA), and plotting was completed using Origin 2024 (OriginLab Corp., Northampton, MA, USA).

3 Results and discussion

3.1 Fluorescence spectrum of SCICHs

Fluorescence spectroscopy is commonly employed to investigate the interactions between small molecules and proteins[26]. The fluorescence spectra of α-amylase with SCIPH, SCITH, and SCINPH at 298, 308, and 318 K were shown in Figure 1. A highest fluorescence peak was observed at approximately 350 nm for all treatments. With increasing hydrolysate concentration, the fluorescence intensity of α-amylase was progressively reduced, indicating a concentration-dependent quenching effect. Under all tested conditions, the highest fluorescence intensity was observed for α-amylase alone, whereas the lowest intensity was detected in the presence of 800 μg/mL SCITH at 318 K. Due to the temperature dependence of fluorescence quenching, Stern-Volmer analysis was performed at various temperatures to calculate quenching constants (Table 1). Combined with the data in Figures 1A$_4$–E$_4$ and Table 1, the Stern-Volmer fitting curves for SCICHs were linear, and the K_{sv} decreased continuously as temperature rose, suggesting that all hydrolysates induced static quenching of α-amylase by all hydrolysates were classified as static quenching.

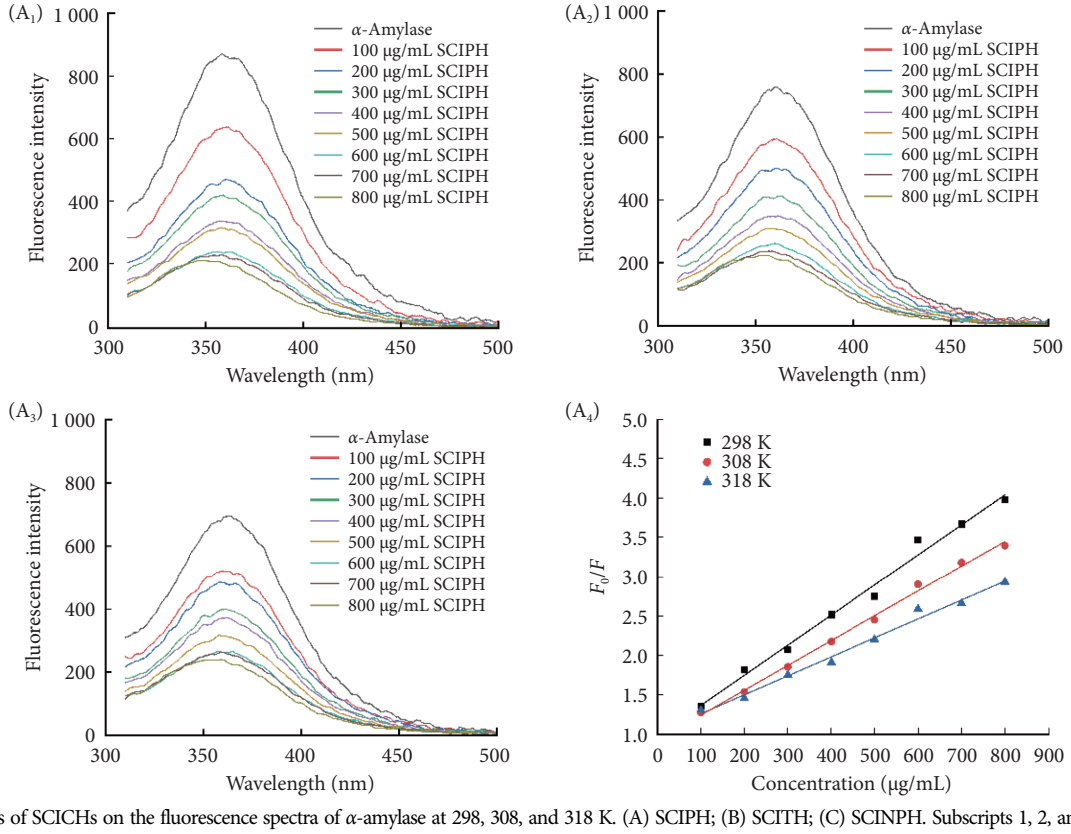


Figure 1 Effects of SCICHs on the fluorescence spectra of α-amylase at 298, 308, and 318 K. (A) SCIPH; (B) SCITH; (C) SCINPH. Subscripts 1, 2, and 3 indicate 298, 308, and 318 K, respectively, while subscript 4 indicates the Stern-Volmer plots.

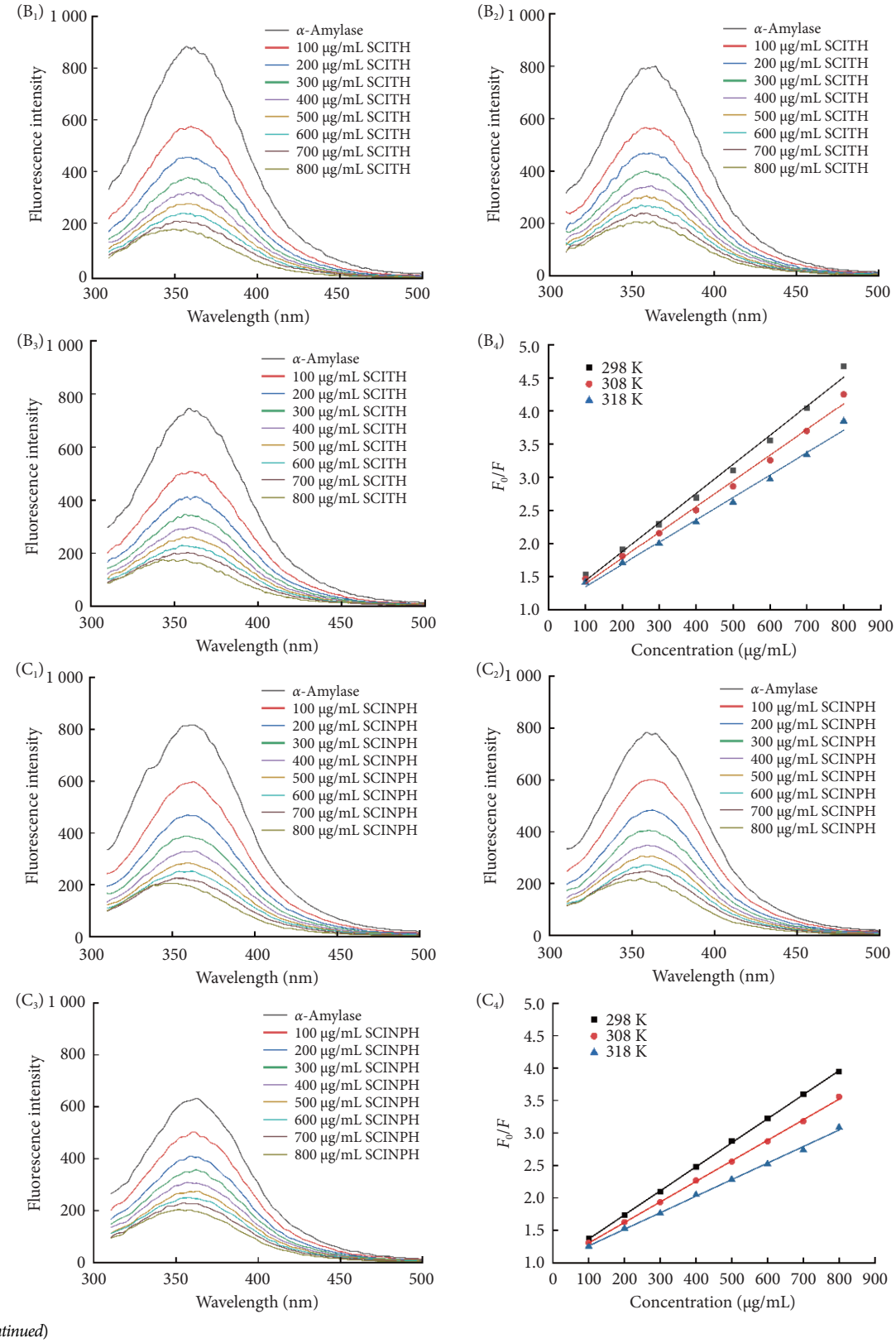


Figure 1 (*Continued*)

The hydrolysate-induced attenuation of fluorescence intensity indicates potential complex formation between collagen hydrolysates and α-amylase. This quenching effect is presumably associated with rearrangement of the enzyme's secondary structure, whereby fluorescent residues are sequestered within the hydrophobic interior, ultimately diminishing fluorescence emission efficiency[37]. Furthermore, the fluorescence quenching efficiency (K_{sv}) declined markedly in the range of 298–318 K, demonstrating the poor thermal stability of the enzyme-hydrolysate complex. Elevated temperature breaks the non-covalent bonds inside the

Table 1 Quenching constants of the interaction between α-amylase and SCICHs.

Sample	T (K)	Equation	R^2	K_{sv} (L/g)	K_q (10^8 L/(g·s))
SCIPH	298	$y = 3.84x + 0.98$	0.986	3.84 ± 0.25	3.84 ± 0.25
	308	$y = 3.17x + 0.92$	0.995	3.17 ± 0.09	3.17 ± 0.09
	318	$y = 2.55x + 1.04$	0.978	2.55 ± 0.04	2.55 ± 0.04
SCITH	298	$y = 4.39x + 0.99$	0.997	4.39 ± 0.15	4.39 ± 0.15
	308	$y = 3.71x + 1.00$	0.994	3.71 ± 0.13	3.71 ± 0.13
	318	$y = 3.16x + 0.92$	0.993	3.16 ± 0.12	3.16 ± 0.12
SCINPH	298	$y = 3.70x + 1.04$	0.993	3.70 ± 0.02	3.70 ± 0.02
	308	$y = 3.38x + 1.02$	0.993	3.38 ± 0.08	3.38 ± 0.08
	318	$y = 2.38x + 1.03$	0.994	2.38 ± 0.17	2.38 ± 0.17

complex, rendering it unable to maintain a stable conformation and eventually dissociate. This increases the effective distance between the fluorophore and quenching center, ultimately attenuating quenching efficiency[28].

In summary, SCICHs associate with α-amylase to generate ground-state complexes, thereby triggering static fluorescence quenching. This binding perturbs the microenvironment of intrinsic fluorophores. Higher temperatures destabilize the intermolecular non-covalent interactions, inducing complex dissociation and consequently weakening the quenching efficacy.

3.2 Secondary structures of SCICHs

CD spectroscopy revealed the conformational transitions in α-amylase induced by SCICHs[29]. The CD spectral profiles of α-amylase after interaction with SCIPH, SCITH, and SCINPH are presented in Figure 2A_1–C_1. The characteristic negative absorption peak near 198 nm corresponds to the α-helix secondary structure of hydrolysates. Concomitant with the increase of SCICHs concentration, the negative ellipticity of the CD spectrum of α-amylase progressively diminished, and SCITH showed the lowest negative ellipticity peak among all hydrolysates. The above findings suggest that the α-helix within α-amylase diminished upon potential binding with SCICHs[30]. The secondary structural composition of α-amylase after treatment with SCIPH, SCITH, and SCINPH is shown in Figure 2A_2–C_2. As the SCICHs concentration increased, the α-helix and random coil relative contents of α-amylase exposed to the three hydrolysates were reduced, whereas the β-sheet relative content was markedly increased. Among all treatment groups, SCITH-treated α-amylase exhibited the lowest α-helix and random coil relative contents and the highest β-sheet relative content. Compared with the control group, SCITH treatment induced pronounced secondary structural rearrangement in α-amylase, as reflected by an increase in β-sheet relative content from 41.48% to 66.05%, together with decreases in α-helix and random coil relative contents from 12.36% to 6.79% and from 30.94% to 7.36%, respectively.

These secondary structural alterations presumably arise from the non-covalent complexation between the peptide and the enzyme, involving hydrogen bonds and hydrophobic interactions[31]. Such interactions disrupt the native conformation of the enzyme, induce rearrangement of its secondary structure, and reduce the binding affinity for the substrate[32–33]. Comparable secondary structural changes were also noted in prior literature. Specifically, Xue et al.[34] reported that phosvitin-derived peptides attach to the non-catalytic domain of α-amylase via non-covalent interactions; this binding remodels the spatial conformation of the enzyme and thereby suppresses its catalytic activity.

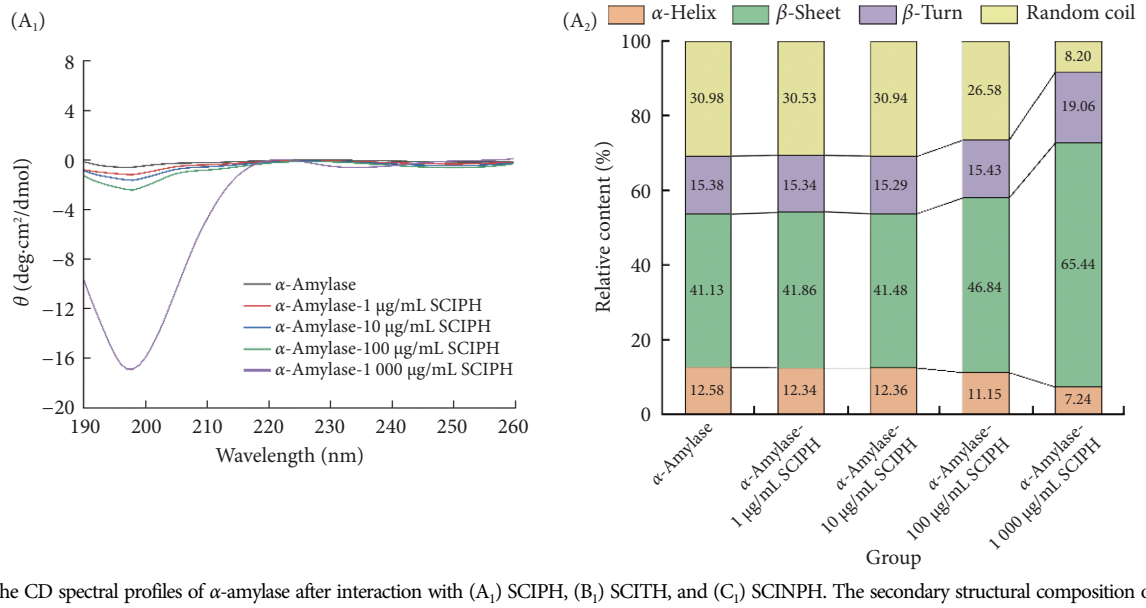


Figure 2 The CD spectral profiles of α-amylase after interaction with (A_1) SCIPH, (B_1) SCITH, and (C_1) SCINPH. The secondary structural composition of α-amylase after treatment with (A_2) SCIPH, (B_2) SCITH, and (C_2) SCINPH.

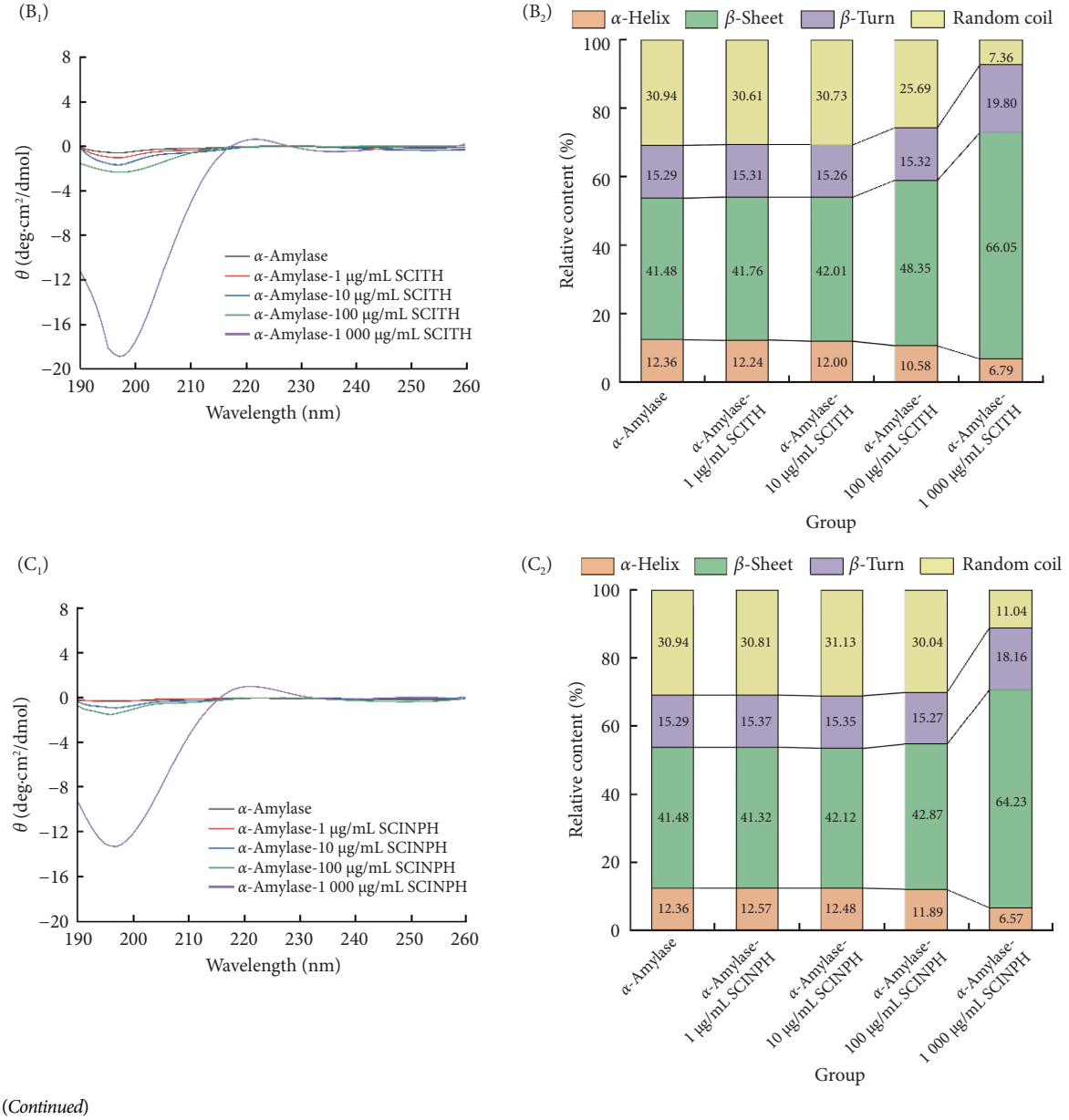


Figure 2 (*Continued*)

In summary, CD spectral data reveal that SCICHs bind to α-amylase via non-covalent interactions, triggering conformational rearrangements in the enzyme's secondary structure. These changes alter the hydrophobic properties of the protein, disrupt the spatial architecture of the active center, hinder substrate binding, and reduce the catalytic capacity of the enzyme.

3.3 Inhibitory effects and mechanisms of SCICHs on α-amylase

3.3.1 *Inhibitory effects of SCICHs on α-amylase activity*

The inhibition rates of different SCICHs on α-amylase are shown in Figure 3. As the SCICHs concentration rose, the inhibitory capacity against α-amylase was also improved. At 100 μg/mL, SCITH demonstrated a significantly higher inhibition rate against α-amylase compared with SCIPH and SCINPH. At 1 000 μg/mL, SCITH displayed the strongest inhibitory activity, achieving an inhibition rate of 64.71% that was comparable to the level of the positive control acarbose (72.06%). As shown in Table 2, SCINPH did not achieve 50% inhibition within the tested concentration range; therefore, its IC_{50} value could not be determined. The IC_{50} of SCIPH was (236.22 ± 0.73) μg/mL. Notably, SCITH exhibited the lowest IC_{50} value among the three hydrolysates, at (87.23 ± 0.46) μg/mL, while the positive control acarbose showed an IC_{50} of (40.54 ± 0.38) μg/mL. Although the IC_{50} value of SCITH was higher than that of acarbose, it falls within the activity range reported for natural α-amylase inhibitory peptides in the literature[35], indicating that SCITH still possesses strong inhibitory activity. The slight gap in inhibitory activity between the two can be attributed to differences in their components, acarbose is a pure compound, whereas SCITH is a complex mixture containing not only active peptides but also non-active components, of which only a portion participates in enzyme inhibition.

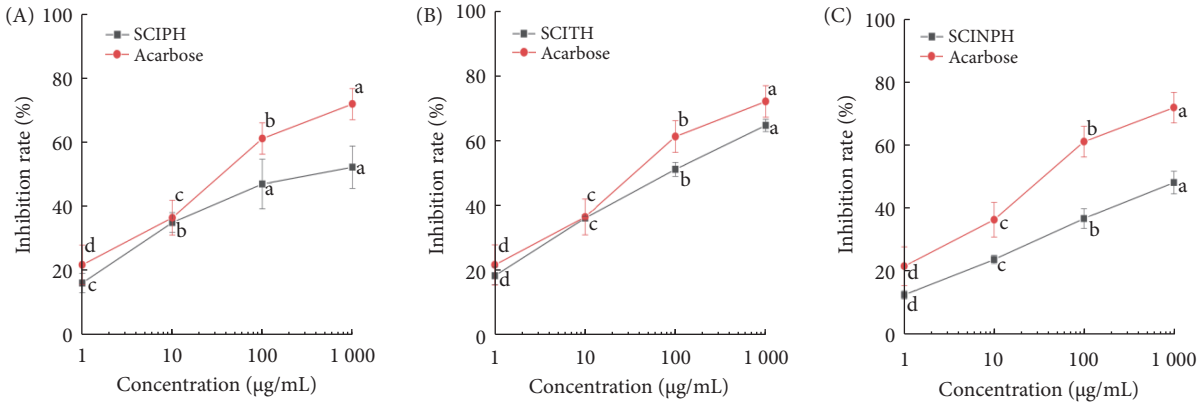


Figure 3 Effects of SCICHs on α-amylase inhibitory activity. (A) SCIPH, (B) SCITH, and (C) SCINPH.

Table 2 IC_{50} values of α-amylase inhibitory activity of SCICHs and acarbose.

Sample	IC_{50} (μg/mL)
SCINPH	
SCIPH	236.22 ± 0.73^{c}
SCITH	87.23 ± 0.46^{b}
Acarbose	40.54 ± 0.38^{a}

Note: Different lowercase letters in the same column indicate significant difference ($P < 0.05$).

The inhibitory effect of SCICHs is derived from its bioactive peptides enriched in Trp, Arg, and Tyr residues. Trp and Tyr dock into the active site of α-amylase through hydrophobic interactions and π-π stacking, competitively blocking the substrate recognition pocket, concurrently, the positively charged Arg group establishes electrostatic interactions with negatively charged catalytic residues (Asp, Glu) in the active cleft, stabilizing the inhibitor enzyme complex and cooperatively lowering the catalytic efficiency[36]. Comparably, Wan et al.[37] reported that *Trachinotus ovatus* hydrolysate-derived functional peptides interact with both the catalytic pocket and allosteric regions of α-amylase through a combination of hydrogen bonds, hydrophobic forces, and π-π stacking, triggering structural rearrangements in the enzyme that culminate in its inactivation. The superior inhibitory activity of SCITH stems from its ability to induce the most significant secondary structural perturbations among the three hydrolysates, as reflected by an increase in β-sheet relative content from 41.48% to 66.05%, a decrease in α-helix relative content from 12.36% to 6.79%, and a decrease in random coil relative content from 30.94% to 7.36%. Such a drastic conformational rearrangement disrupts the spatial architecture of the catalytic center, consequently impairing substrate binding and catalytic efficiency. In addition, SCITH displayed the lowest K_i and K_{is} values (Table 3), reflecting its highest affinity toward both the free enzyme and the enzyme-substrate complex. Similarly, Xu et al.[38] reported that trypsin hydrolysate from salmon bone released peptides that specifically bound to α-amylase and exerted mixed-type inhibition.

Table 3 Inhibition constants and inhibition types of α-amylase by SCICHs.

Sample	K_i (mg/mL)	K_{is} (mg/mL)	Inhibition type
SCINPH	1.36	6.92	Mixed inhibition
SCIPH	0.99	5.27	Mixed inhibition
SCITH	0.91	3.94	Mixed inhibition

Collectively, the enzyme inhibitory activity data demonstrated that the bioactive peptides in SCICHs bind to the active site of α-amylase through intermolecular non-covalent forces and effectively suppress the catalytic activity of α-amylase.

3.3.2 *Mode and type of inhibition*

The inhibitory kinetics of α-amylase were determined using the Lineweaver-Burk double reciprocal plot method, as shown in Figures 4A–C, the plots derived at varying hydrolysate

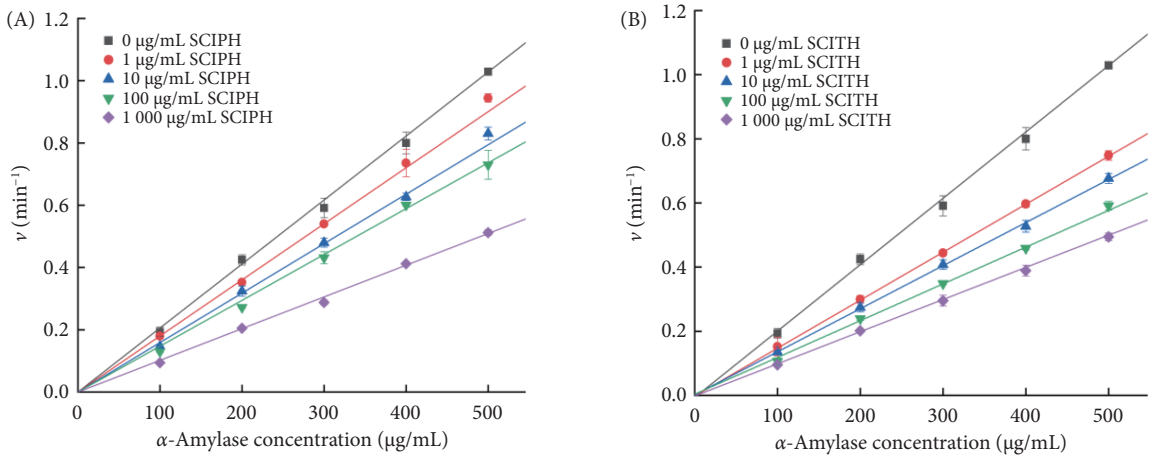


Figure 4 Inhibition kinetics curves and inhibition types of α-amylase by SCICHs. Kinetic curves of (A) SCIPH, (B) SCITH, and (C) SCINPH inhibiting α-amylase. Lineweaver-Burk plots of mixed inhibition of α-amylase by (D) SCIPH, (E) SCITH and (F) SCINPH.

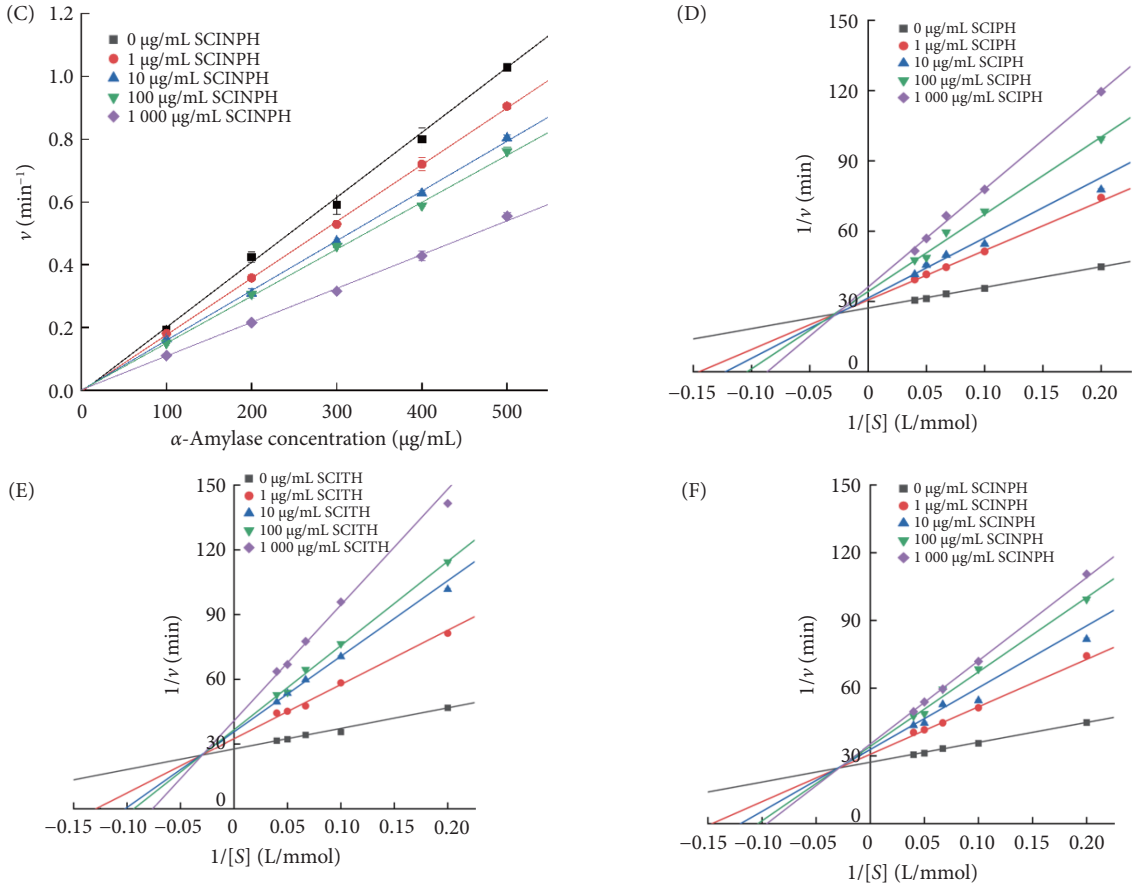


Figure 4 (*Continued*)

concentrations intersected at the origin, and the slope values declined as the inhibitor concentration rose, indicating a concentration-dependent inhibitory effect. Such findings demonstrate that the suppressive effect exerted by the hydrolysates on α-amylase was non-permanent, with no irreversible loss of catalytic function being observed[39].

To elucidate the inhibitory mode of three sea cucumber intestinal hydrolysates toward α-amylase, kinetic characterization was performed using the Lineweaver-Burk approach. Enzyme inhibition theory distinguishes four categories of inhibitor action: competitive, non-competitive, uncompetitive, and mixed, which differ fundamentally in binding loci, kinetic behavior, and reciprocal plot patterns[40]. As shown in Figures 4D–F, fitted lines for various hydrolysate concentrations intersected in the second quadrant, characteristic of mixed-type inhibition, indicating SCICHs bind both free enzyme and enzyme-substrate complex. The constants K_i (reflecting affinity for the free enzyme) and K_{is} (reflecting affinity for the enzyme-substrate complex) were subsequently derived and tabulated in Table 3. Kinetic data indicated that SCICHs exhibited a lower K_i than K_{is}, implying concurrent interaction with both free α-amylase and the enzyme-substrate complex, yet with markedly stronger binding to the former. Comparative evaluation revealed SCITH as possessing the lowest K_i and K_{is} values across all samples, signifying the highest affinity for α-amylase and the greatest inhibitory potency.

Similarly, Xu et al.[38] reported that proteolytic products from salmon fish bones elicited mixed inhibition of α-amylase. These substances could effectively bind to the amino acid residues (e.g., Asp206 and Trp203) at the calcium-binding sites within α-amylase, thereby eliciting conformational alterations in the enzyme. Zhong et al.[41] reported that oyster peptide-anthocyanin complexes act as mixed-type inhibitors against α-amylase. Such dual binding toward free enzymes and enzyme-substrate complexes disrupts the internal microenvironment and spatial structure of the enzyme, which accounts for its inhibitory performance. While no single functional peptide sequence was characterized in their work, the peptide-enzyme binding interaction distorts α-amylase conformation and weakens its catalytic activity.

4 Conclusions

In the present investigation, three collagen hydrolysates exhibiting α-amylase inhibitory capacity were enzymatically generated from sea cucumber intestinal tissues. Fluorescence and CD spectroscopy results showed that they could bind to α-amylase in a concentration-dependent manner, inducing its secondary structure changes. Inhibitory rate analysis showed that SCITH exhibited the optimal α-amylase inhibitory effect, with an inhibition rate of 64.71% at 1 000 μg/mL, close to the positive control acarbose. According to kinetic measurements, SCICHs exerted reversible mixed-type inhibition against α-amylase, as it was able to interact with both the catalytic pocket of α-amylase and the enzyme-substrate complex simultaneously. In summary, SCICHs act as a natural and safe α-amylase inhibitor, which not only enables high-value processing and resource utilization of by-products but also possesses promising application prospects as natural α-amylase inhibitors.

Declaration of competing interest

The authors declare no conflicts of interest.

Acknowledgments

This work was supported by the National Natural Science Foundation of China (32302072), Liaoning Provincial Science and Technology Programme Joint Programme (2024JH2/102600100) and the Fundamental Research Funds for the Central Universities (044420250059).

Author contributions

Zhe Xu: Writing–review & editing, writing–original draft, methodology, investigation, funding acquisition, formal analysis. Tengfei Li: Writing–review & editing, writing–original draft, methodology, investigation, formal analysis. Zijin Qin: Writing–review & editing, methodology, formal analysis. Shuyu Zhou: Conceptualization, methodology, conceptualization. Jianbo Sun: Software, methodology. Xuguang Mo: Software, methodology, conceptualization. Fuzhen Wang: Software, methodology, conceptualization. Tingting Li: Writing–review & editing, writing–original draft, methodology, funding acquisition, conceptualization.

Data availability

Data will be made available on request.

References

[1] S. B. Heymsfield, D. L. Longo, T. A. Wadden, et al., Pathophysiology and management of obesity, N. Engl. J. Med. 376(3) (2017) 254–266. https://doi.org/10.1056/NEJMra1514009.

[2] N. H. Phelps, R. K. Singleton, B. Zhou, et al., Worldwide trends in underweight and obesity from 1990 to 2022: a pooled analysis of 3 663 population-representative studies with 222 million children, adolescents, and adults, Lancet 403(10431) (2024) 1027–1050. https://doi.org/10.1016/s0140-6736(23)02750-2.

[3] Z. Li, B. Zhang, N. Wang, et al., A novel peptide protects against diet-induced obesity by suppressing appetite and modulating the gut microbiota, Gut 72(4) (2023) 686–698. https://doi.org/10.1136/gutjnl-2022-328035.

[4] Š. Janeček, B. Svensson, E. A. MacGregor, et al., α-Amylase: an enzyme specificity found in various families of glycoside hydrolases, Cell. Mol. Life Sci. 71(7) (2013) 1149–1170. https://doi.org/10.1007/s00018-013-1388-z.

[5] E. Valencia-Mejía, K. A. Batista, J. J. A. Fernández, et al., Antihyperglycemic and hypoglycemic activity of naturally occurring peptides and protein hydrolysates from easy-to-cook and hard-to-cook beans (*Phaseolus vulgaris* L), Food Res. Int. 121 (2019) 238–246. https://doi.org/10.1016/j.foodres.2019.03.043.

[6] F. M. de Matos, J. T. J. G. de Lacerda, G. Zanetti, et al., Production of black cricket protein hydrolysates with α-amylase, α-glucosidase and angiotensin I-converting enzyme inhibitory activities using a mixture of proteases, Biocatal. Agric. Biotechnol. 39 (2022) 102276. https://doi.org/10.1016/j.bcab.2022.102276.

[7] G. Q. Yuan, W. W. Li, Y. X. Pan, et al., Shrimp shell wastes: optimization of peptide hydrolysis and peptide inhibition of α-amylase, Food Chem. 25 (2018) 52–60. https://doi.org/10.1016/j.fbio.2018.07.008.

[8] O. Sintsova, D. Popkova, A. Kalinovskii, et al., Control of postprandial hyperglycemia by oral administration of the sea anemone mucus-derived α-amylase inhibitor (magnificamide), Biomed. Pharmacother. 168 (2023) 115743. https://doi.org/10.1016/j.biopha.2023.115743.

[9] Y. Y. Tian, S. W. Hu, H. Xu, et al., Long-chain bases from *Cucumaria frondosa* inhibit adipogenesis and regulate lipid metabolism in 3T3-L1 adipocytes, Food Sci. Biotechnol. 25(6) (2016) 1753–1760. https://doi.org/10.1007/s10068-016-0267-4.

[10] P. Lin, N. Shen, F. Yin, et al., Sea cucumber-derived compounds for treatment of dyslipidemia: a review, Front. Pharmacol. 13 (2022) 1000315. https://doi.org/10.3389/fphar.2022.1000315.

[11] Y. Khotimchenko, Pharmacological potential of sea cucumbers, Int. J. Mol. Sci. 19(5) (2018) 1342. https://doi.org/10.3390/ijms19051342.

[12] Z. Q. Lu, N. Sun, L. Dong, et al., Production of bioactive peptides from sea cucumber and its potential health benefits: a comprehensive review, J. Agric. Food Chem. 70(25) (2022) 7607–7625. https://doi.org/10.1021/acs.jafc.2c02696.

[13] Y. W. Shou, C. Feng, Q. P. Lu, et al., Research progress on the chemical components and biological activities of sea cucumber polypeptides, Front. Pharmacol. 14 (2023) 1290175. https://doi.org/10.3389/fphar.2023.1290175.

[14] S. Bordbar, F. Anwar, N. Saari, et al., High-value components and bioactives from sea cucumbers for functional foods: a review, Mar. Drugs 9(10) (2011) 1761. https://doi.org/10.3390/md9101761.

[15] G. Chen, X. F. Ge, Y. Sun, et al., Identification of two novel α-amylase inhibitory activity peptide from Russian sea cucumber body wallprotein hydrolysate, Int. J. Biol. Macromol. 295 (2025) 139499. https://doi.org/10.1016/j.ijbiomac.2025.139499.

[16] S. Lin, Y. P. Xue, E. San, et al., Extraction and characterization of pepsin soluble collagen from the body wall of sea cucumber acaudina ieucoprocta, J. Aquat. Food Prod. Technol. 26(5) (2017) 502–515. https://doi.org/10.1080/10498850.2016.1222560.

[17] M. L. Yang, Z. Xu, D. Wu, et al., Characterizations and the mechanism underlying osteogenic activity of peptides from enzymatic hydrolysates of *Stichopus japonicus*, J. Agric. Food Chem. 69(51) (2021) 15611–15623. https://doi.org/10.1021/acs.jafc.1c06028.

[18] Y. F. Duan, D. Deng, X. Yang, et al., Bovine liver hydrolysates based on six proteases: physicochemical properties, emulsification characteristics, antioxidant capacity assessment, and peptide identification, LWT-Food Sci. Technol. 208 (2024) 116718. https://doi.org/10.1016/j.lwt.2024.116718.

[19] Y. Q. Lu, W. Y. Zhou, Y. Feng, et al., Acteoside and acyl-migrated acteoside, compounds in Chinese kudingcha tea, inhibit α-amylase *in vitro*, J. Med. Food 20(6) (2017) 577–585. https://doi.org/10.1089/jmf.2016.3910.

[20] B. T. Liu, Y. L. Zhuang, L. P. Sun, Identification and characterization of the peptides with calcium-binding capacity from tilapia (*Oreochromis niloticus*) skin gelatin enzymatic hydrolysates, J. Food Sci. 85(1) (2019) 114–122. https://doi.org/10.1111/1750-3841.14975.

[21] G. W. Zhang, Y. D. Ma, Mechanistic and conformational studies on the interaction of food dye amaranth with human serum albumin by multispectroscopic methods, Food Chem. 136(2) (2013) 442–449. https://doi.org/10.1016/j.foodchem.2012.09.026.

[22] X. Q. Wu, M. M. Hu, X. Hu, et al., Inhibitory mechanism of epicatechin gallate on α-amylase and α-glucosidase and its combinational effect with acarbose or epigallocatechin gallate, J. Mol. Liq. 290 (2019) 111202. https://doi.org/10.1016/j.molliq.2019.111202.

[23] A. S. Naganarasimha, S. M. Patil, R. Ramu, et al., Coconut milk-derived bioactive peptides as multifunctional agents against hyperglycemia, oxidative stress, and glycation: an integrated experimental and computational study, Int. J. Mol. Sci. 27(1) (2025) 360–391. https://doi.org/10.3390/ijms27010360.

[24] N. Cardullo, V. Muccilli, L. Pulvirenti, et al., *C*-Glucosidic ellagitannins and galloylated glucoses as potential functional food ingredients with anti-diabetic properties: a study of α-glucosidase and α-amylase inhibition, Food Chem. 313 (2020) 126099. https://doi.org/10.1016/j.foodchem.2019.126099.

[25] A. A. Anigboro, O. J. Avwioroko, O. Akeghware, et al., Anti-obesity, antioxidant and *in silico* evaluation of *Justicia carnea* bioactive compounds as potential inhibitors of an enzyme linked with obesity: insights from kinetics, semi-empirical quantum mechanics and molecular docking analysis, Biophys. Chem. 274 (2021) 1071–1085. https://doi.org/10.1016/j.bpc.2021.106607.

[26] A. Yammine, J. Gao, A. Kwan, et al., Tryptophan fluorescence quenching assays for measuring protein-ligand binding affinities: principles and a practical guide, Bio-protocol 9(11) (2019) 3253. https://doi.org/10.21769/BioProtoc.3253.

[27] Y. F. Deng, R. E. Aluko, Q. Jin, et al., Inhibitory activities of baicalin against renin and angiotensin-converting enzyme, Pharm. Biol. 50(4) (2011) 401–406. https://doi.org/10.3109/13880209.2011.608076.

[28] Y. X. Zheng, J. H. Tian, W. H. Yang, et al., Inhibition mechanism of ferulic acid against α-amylase and α-glucosidase, Food Chem. 317 (2020) 126346. https://doi.org/10.1016/j.foodchem.2020.126346.

[29] R. Hussain, C. S. Hughes, G. Siligardi, et al., Correction to: enzyme-ligand interaction monitored by synchrotron radiation circular dichroism, Meth. Mol. Biol. 2089 (2020) 87–118. https://doi.org/10.1007/978-1-0716-0163-1_9.

[30] S. W. Liu, F. N. Meng, S. Guo, et al., Inhibition of α-amylase digestion by a lonicera caerulea berry polyphenol starch complex revealed via multi-spectroscopic and molecular dynamics analyses, Int. J. Biol. Macromol. 260 (2024) 129573. https://doi.org/10.1016/j.ijbiomac.2024.129573.

[31] J. Li, M. Y. Ma, F. Liang, et al., Multi-target antidiabetic peptides from highland barley (Qingke): identification, molecular docking, and inhibitory mechanisms against α-amylase, α-glucosidase, and DPP-IV, Food Chem. 508 (2026) 148412. https://doi.org/10.1016/j.foodchem.2026.148412.

[32] Z. X. Han, W. W. Ren, X. J. Liu, et al., Hypoglycemic activity of immature persimmon (*Diospyros kaki* Thunb) extracts and its inhibition mechanism for α-amylase and α-glucosidase, Int. J. Biol. Macromol. 257 (2024) 128616. https://doi.org/10.1016/j.ijbiomac.2023.128616.

[33] H. Y. Shen, J. Wang, J. F. Ao, et al., Structure-activity relationships and the underlying mechanism of α-amylase inhibition by hyperoside and quercetin: multi-spectroscopy and molecular docking analyses, Spectrochim. Acta A Mol. Biomol. Spectrosc. 285 (2023) 121797. https://doi.org/10.1016/j.saa.2022.121797.

[34] T. R. Xue, W. Zhao, C. Y. Hao, et al., Two novel phosvitin peptides FGTEPDAK and IWGR: the dual effects and associated mechanisms for inhibiting α-amylase and alleviating insulin resistance in IR-HepG2 cells, Food Chem. 475 (2025) 143314. https://doi.org/10.1016/j.foodchem.2025.143314.

[35] F. Ramirez-Lozano, J. Contreras, A. Alfaro-Diaz, et al., Peptides from 'Vaina Morada' black bean inhibit α-amylase and α-glucosidase: a combined *in silico-in vitro* study, Foods 14(22) (2025) 3847–3868. https://doi.org/10.3390/foods14223847.

[36] Z. Xu, X. Yan, Z. J. Qin, et al., Preparation of sea cucumber collagen hydrolysate and its inhibitory effect on α-glucosidases, Food Chem.: X 33 (2026) 103472. https://doi.org/10.1016/j.fochx.2025.103472.

[37] P. Wan, B. N. Cai, H. Chen, et al., Antidiabetic effects of protein hydrolysates from *Trachinotus ovatus* and identification and screening of peptides with α-amylase and DPP-IV inhibitory activities, Curr. Res. Food Sci. 6 (2023) 100446. https://doi.org/10.1016/j.crfs.2023.100446.

[38] Z. Xu, S. Y. Han, N. Cui, et al., Identification and characterization of a calcium-binding peptide from salmon bone for the targeted inhibition of α-amylase in digestion, Food Chem.: X 22 (2024) 101352. https://doi.org/10.1016/j.fochx.2024.101352.

[39] R. Xing, A. P. Zheng, F. Wang, et al., Functionality study of $Na_6PMo_{11}FeO_{40}$ as a mushroom tyrosinase inhibitor, Food Chem. 175 (2015) 292–299. https://doi.org/10.1016/j.foodchem.2014.11.157.

[40] T. Oyama, S. Takahashi, A. Yoshimori, et al., Discovery of a new type of scaffold for the creation of novel tyrosinase inhibitors, Bioorg. Med. Chem. 24(18) (2016) 4509–4515. https://doi.org/10.1016/j.bmc.2016.07.060.

[41] K. C. Zhong, M. L. Jiang, W. H. Cao, et al., Interaction between oyster peptides and anthocyanins: stability improvement, structure changes and α-amylase and α-glucosidase inhibition effect, LWT-Food Sci. Technol. 221 (2025) 117592. https://doi.org/10.1016/j.lwt.2025.117592.